

# Bipolar thermoelectric effect in a serially coupled quantum dot system

David M.-T. Kuo<sup>1†</sup>, and Yia-chung Chang<sup>2\*</sup>

<sup>1</sup>*Department of Electrical Engineering and Department of Physics,  
National Central University, Chungli, 320 Taiwan and*

<sup>2</sup>*Research Center for Applied Sciences, Academic Sinica, Taipei, 115 Taiwan*

(Dated: April 18, 2022)

The Seebeck coefficient (S) of a serially coupled quantum dot (SCQD) junction system is theoretically studied via a two-level Anderson model. A change of sign in S with respect to temperature is found, which arises from the competition between tunneling currents due to electrons and holes (i.e, bipolar tunneling effect). The change of sign in S implies that one can vary the equilibrium temperature to produce thermoelectric current in either the forward or reverse direction, leading to a bipolar thermoelectric effect. For the case of two parallel SCQDs, we also observe the oscillatory behavior of S with respect to temperature.

Owing to energy and environment issues, it has become important to consider novel applications related to the thermal properties of materials. Many considerable studies have been devoted to seeking efficient thermoelectric materials because there exist potential applications of solid state thermal devices such as coolers and power generators.<sup>1-9</sup> A quantum dot-(QD) based thermal device was also predicted to have more pronounced enhancement in energy conversion.<sup>9</sup> Recently, some theoretical efforts have focused on the thermoelectric effects in nanostructure junctions,<sup>10-13</sup> however, not many works have paid attention to the thermoelectric effects of a serially coupled quantum dot (SCQD) junction, which exhibits features of current rectification due to spin blockade, negative differential conductance, non-thermal broadening of electrical conductance, and coherent tunneling (for identical QDs) in the Coulomb blockade regime.<sup>14</sup> Our recent work has described these observed phenomena in a unified theory.<sup>15</sup> Based on our previous work, we find that the Seebeck coefficient of SCQDs exhibits a behavior of sign change with respect to temperature arising from electron Coulomb interactions.

Using the Keldysh-Green's function technique,<sup>15</sup> we can express (up to the second order in the interdot coupling,  $t_c$ ) the tunneling current through a serially coupled QDs connected to metallic electrodes (shown in the inset of Fig. 1)

$$J = \frac{2e}{h} \int d\epsilon \mathcal{T}(\epsilon) [f_L(\epsilon) - f_R(\epsilon)] \quad (1)$$

where  $\mathcal{T}(\epsilon) \equiv \Gamma_L(\epsilon)\Gamma_R(\epsilon)(\mathcal{A}_{12} + \mathcal{A}_{21})/2$  is the transmission factor.  $\Gamma_{\ell=L,R}(\epsilon)$  denote the tunnel rate from the left electrode to dot A and the right electrode to dot B.  $f_{L(R)}(\epsilon) = 1/[e^{(\epsilon - \mu_{L(R)})/k_B T_{L(R)}} + 1]$  denotes the Fermi distribution function for the left (right) electrode. The chemical potential difference between these two electrodes is related to  $\mu_L - \mu_R = e\Delta V$ .  $T_{L(R)}$  denotes the equilibrium temperature of the left (right) electrode.  $e$  and  $h$  denote the electron charge and Plank's constant, respectively. For simplicity, we consider wide-band limit that is  $\Gamma_{\ell}(\epsilon) = \Gamma_{\ell}$ .  $\mathcal{A}_{\ell,j}$  denotes the spectral density, which can be calculated by one particle off diagonal Green's function.<sup>15</sup> In the atomic limit, we have

$$\mathcal{A}_{\ell,j}(\epsilon) = t_c^2 \sum_m p_m / |\Pi_m|^2; \quad (\ell \neq j), \quad (2)$$

where the numerators denote probability factors for various charge configurations, and they are  $p_1 = (1 - N_{\ell,\bar{\sigma}})(1 - N_{j,\sigma} - N_{j,\bar{\sigma}} + c_j)$ ,  $p_2 = (1 - N_{\ell,\bar{\sigma}})(N_{j,\bar{\sigma}} - c_j)$ ,  $p_3 = (1 - N_{\ell,\bar{\sigma}})(N_{j,\sigma} - c_j)$ ,  $p_4 = (1 - N_{\ell,\bar{\sigma}})c_j$ ,  $p_5 = N_{\ell,\bar{\sigma}}(1 - N_{j,\sigma} - N_{j,\bar{\sigma}} + c_j)$ ,  $p_6 = N_{\ell,\bar{\sigma}}(N_{j,\bar{\sigma}} - c_j)$ ,  $p_7 = N_{\ell,\bar{\sigma}}(N_{j,\sigma} - c_j)$ , and  $p_8 = N_{\ell,\bar{\sigma}}c_j$ . The denominators for the eight configurations are (i)  $\Pi_1 = \mu_{\ell}\mu_j - t_c^2$  with both dots empty, (ii)  $\Pi_2 = (\mu_{\ell} - U_{\ell,j})(\mu_j - U_j) - t_c^2$ , with dot A empty and dot B filled by one electron with spin  $\bar{\sigma}$ , (iii)  $\Pi_3 = (\mu_{\ell} - U_{\ell,j})(\mu_j - U_{j,\ell}) - t_c^2$  with dot A empty and dot B filled by one electron with spin  $\sigma$ , (iv)  $\Pi_4 = (\mu_{\ell} - 2U_{\ell,j})(\mu_j - U_j - U_{j,\ell}) - t_c^2$  with dot A is empty and dot B filled by two electrons, (v)  $\Pi_5 = (\mu_{\ell} - U_{\ell})(\mu_j - U_{j,\ell}) - t_c^2$  with dot B empty and dot A filled by one electron with spin  $\bar{\sigma}$ , (vi)  $\Pi_6 = (\mu_{\ell} - U_{\ell} - U_{\ell,j})(\mu_j - U_j - U_{j,\ell}) - t_c^2$  with both dots filled by one electron with spin  $\bar{\sigma}$ ,  $\Pi_7 = (\mu_{\ell} - U_{\ell} - U_{\ell,j})(\mu_j - 2U_{j,\ell}) - t_c^2$  with dot A filled by one electron with spin  $\bar{\sigma}$  and dot B filled by one electron with spin  $\sigma$ , and (viii)  $\Pi_8 = (\mu_{\ell} - U_{\ell} - 2U_{\ell,j})(\mu_j - U_j - 2U_{j,\ell}) - t_c^2$  with dot A filled by one electron with spin  $\bar{\sigma}$  and dot B filled by two electrons.  $\mu_{\ell} = \epsilon - E_{\ell} + i\Gamma_{\ell}$ . The notations  $E_{\ell}$ ,  $U_{\ell}$ , and  $U_{\ell,j}$  denote, respectively, the energy levels of dots, intradot Coulomb interactions, and interdot Coulomb interactions.  $t_c$  denotes the electron hopping strength between two dots.

The probability factor for all channels of Eq. (2) are determined by the thermally averaged one-particle occupation number and two-particle correlation functions, which can be obtained by solving the lesser Green's functions. We have  $N_{\ell,\sigma} = -(1/\pi) \int d\epsilon f_{\ell}(\epsilon) \text{Im} G_{\ell,\sigma}^r(\epsilon)$ , and  $c_{\ell} = -(1/\pi) \int d\epsilon f_{\ell}(\epsilon) \text{Im} G_{\ell,\ell}^r(\epsilon)$ , where the retarded Green functions  $G_{\ell,\sigma}^r(\epsilon)$  and  $G_{\ell,\ell}^r(\epsilon)$  are, respectively, given by

$$\begin{aligned} & G_{\ell,\sigma}^r(\epsilon) \quad (3) \\ &= \frac{p_1}{\mu_{\ell} - t_c^2/\mu_j} + \frac{p_2}{(\mu_{\ell} - U_{\ell,j}) - t_c^2/(\mu_j - U_j)} \\ &+ \frac{p_3}{(\mu_{\ell} - U_{\ell,j}) - t_c^2/(\mu_j - U_{j,\ell})} \end{aligned}$$

$$\begin{aligned}
& + \frac{p_4}{(\mu_\ell - 2U_{\ell,j}) - t_c^2/(\mu_j - U_j - U_{j,\ell})} \\
& + \frac{p_5}{(\mu_\ell - U_\ell) - t_c^2/(\mu_j - U_{j,\ell})} \\
& + \frac{p_6}{(\mu_\ell - U_\ell - U_{\ell,j}) - t_c^2/(\mu_j - U_j - U_{j,\ell})} \\
& + \frac{p_7}{(\mu_\ell - U_\ell - U_{\ell,j}) - t_c^2/(\mu_j - 2U_{j,\ell})} \\
& + \frac{p_8}{(\mu_\ell - U_\ell - 2U_{\ell,j}) - t_c^2/(\mu_j - U_j - 2U_{j,\ell})},
\end{aligned}$$

and

$$\begin{aligned}
& G_{\ell,\ell}^r(\epsilon) \\
& = \frac{p_5}{(\mu_\ell - U_\ell) - t_c^2/(\mu_j - U_{j,\ell})} \\
& + \frac{p_6}{(\mu_\ell - U_\ell - U_{\ell,j}) - t_c^2/(\mu_j - U_j - U_{j,\ell})} \\
& + \frac{p_7}{(\mu_\ell - U_\ell - U_{\ell,j}) - t_c^2/(\mu_j - 2U_{j,\ell})} \\
& + \frac{p_8}{(\mu_\ell - U_\ell - 2U_{\ell,j}) - t_c^2/(\mu_j - U_j - 2U_{j,\ell})}.
\end{aligned} \tag{4}$$

Occupation numbers of Eqs. (3) and (4) should be solved self-consistently. Note that in the absence of  $t_c$  the expressions of Eqs. (3) and (4) can also be found in our previous works.<sup>16,17</sup> In the linear response regime, Eq. (2) can be rewritten as

$$J = \mathcal{L}_{11}\Delta V + \mathcal{L}_{12}\Delta T, \tag{5}$$

where  $\Delta T = T_L - T_R$  is the temperature difference across the junction. Coefficients in Eq. (5) are given by

$$\begin{aligned}
\mathcal{L}_{11} & = \frac{2e^2}{h} \int d\epsilon \mathcal{T}(\epsilon) \left( \frac{\partial f(\epsilon)}{\partial E_F} \right)_T, \\
\mathcal{L}_{12} & = \frac{2e}{h} \int d\epsilon \mathcal{T}(\epsilon) \left( \frac{\partial f(\epsilon)}{\partial T} \right)_{E_F}.
\end{aligned} \tag{6}$$

Here  $\mathcal{T}(\epsilon)$  and  $f(\epsilon) = 1/[e^{(\epsilon - E_F)/k_B T} + 1]$  are evaluated at thermal equilibrium. If the system is in an open circuit, the electrochemical potential ( $\Delta V$ ) will be established in response to a temperature gradient; this electrochemical potential is known as the Seebeck voltage. The Seebeck coefficient is defined as  $S = \Delta V/\Delta T = -\mathcal{L}_{12}/\mathcal{L}_{11}$ , where  $\mathcal{L}_{11}$  denotes the electrical conductance,  $G_e$ .

Using the following physical parameters:  $U_\ell = U_0 = 30\Gamma_0$ ,  $U_{12} = 10\Gamma_0$ , and  $\Gamma_L = \Gamma_R = 1\Gamma_0$ , where the average tunneling rate  $\Gamma_0$  has been used as a convenient energy unit, we numerically calculate the thermoelectric coefficients  $\mathcal{L}_{11}$  and  $\mathcal{L}_{12}$ . Figure 1 shows the electrical conductance  $G_e$  and Seebeck coefficient ( $S$ ) as a function of temperature at nonzero orbital offset ( $E_1 - E_2 = \Delta E \neq 0$ ). For the case of  $E_2 = E_F - U_0$  and  $\Delta E = U_2 - U_{12}$ , the electrons injected by a small bias can only tunnel through the the spin singlet state

of the SCQD. This is the so-called "spin blockade" effect of the SCQD.<sup>14,15,18,19</sup> The electrical conductance is suppressed when  $E_2$  deviates from the resonance condition with  $\Delta E = U_2 - U_{12}$ , and we observe that there is a zero-crossing temperature  $T_0$  for the Seebeck coefficient, i.e,  $S(T) = 0$  at  $T = T_0$ . A zero Seebeck coefficient  $S(T_0)$  indicates that the current arising from the temperature gradient can be self-consistently balanced without electrochemical potential. The negative  $S$  indicates that electron carriers of the left (hot) electrode diffuse into the right (cold) electrode via the resonant channels above  $E_F$ , the negative  $\Delta V$  is built up to reach the condition of  $J = 0$  at open circuit [see eq. (5)]. For example, the curve of  $E_1 = E_F - 10\Gamma_0$  and  $E_2 = E_F - 30\Gamma_0$  has a negative Seebeck coefficient. Note that the resonant channel  $E_1 + U_{12} = E_2 + U_2$  [see the inset of Fig. 1(b)] has a zero contribution in  $S$ . On the other hand, the Seebeck coefficient is positive when holes of the right electrode diffuse into the left electrode via the resonant channels below  $E_F$ . Here, we define the unoccupied states below  $E_F$  as holes. Consequently, the change in sign of  $S$  is attributed to the competition between tunneling currents due to electrons and holes. To further clarify the mechanism of  $S$  in sign change with respect to temperature, we consider the case of zero orbital offset for simplicity.

Figure 2(a) shows the Seebeck coefficient as a function of temperature for various electron Coulomb interactions with  $E_\ell = E_0 = E_F - 10\Gamma_0$ . In the noninteracting case ( $U_\ell = U_{\ell,j} = 0$ ),  $S$  is always positive (see dash-dotted curve). This is because the tunneling process is dominated by holes of the hot electrode (left electrode) diffusing into the cold electrode (right electrode) through a level  $E_0$  below  $E_F$  in the weak  $t_c$  limit. To reveal the mechanism of sign change in the Seebeck coefficient for the interacting case (as shown by solid curves in Fig. 2), we analyze the contributions associated with different poles described in eq. (2). In the weak  $t_c$  limit, there are six poles associated with the left dot for the spectral density:  $\epsilon = E_0$ ,  $\epsilon = E_0 + U_{12}$ ,  $\epsilon = E_0 + 2U_{12}$ ,  $\epsilon = E_0 + U_0$ ,  $\epsilon = E_0 + U_0 + U_{12}$ , and  $\epsilon = E_0 + U_0 + 2U_{12}$ . In addition, we also find that only four channels ( $p_1$ ,  $p_3$ ,  $p_6$ , and  $p_8$ ) have high probability weighting. They correspond, respectively, to the resonant channels  $\epsilon = E_0$ ,  $\epsilon = E_0 + U_{12}$ ,  $\epsilon = E_0 + U_0 + U_{12}$ , and  $\epsilon = E_0 + U_0 + 2U_{12}$ . When  $U_{12} = 10\Gamma_0$ , the  $p_3$  channel does not contribute to  $S$  because its pole location is aligned with the Fermi level, i.e,  $E_0 + U_{12} = E_F$ . The strengths of  $p_1$ ,  $p_6$ , and  $p_8$  for  $U_{12} = 10\Gamma_0$  as functions of temperature are shown in Fig. 2(b). The hole contribution is given by  $p_1$ , which leads to a positive contribution to  $S$ . The electron contribution is governed by  $p_6$  and  $p_8$ , which correspond to resonant channels with energy above  $E_F$ , providing a negative contribution to the Seebeck coefficient. Consequently, the change in sign of  $S$  results from the interplay between the competition of electron and hole flows. The behavior of the Seebeck coefficient near the zero-crossing temperature  $T_0$  is linear. When the equilibrium temperature is away from  $T_0$ , the sign change in the Seebeck coefficient

indicates that one can produce thermoelectric current in either the forward or reverse direction, leading to a bipolar thermoelectric effect. On the basis of the closed form solutions of transmission factors and Green's functions, we can solve  $\mathcal{L}_{11}$  and  $\mathcal{L}_{12}$  in terms of polygamma functions to find  $T_0$  accurately. We find that  $T_0$  is mainly dominated by  $U_\ell$  in the atomic limit ( $t_c/U_\ell \ll 1$ ), and  $T_0$  increases with increasing  $U_\ell$  at fixed  $E_\ell$ , but is insensitive to the variation in  $U_{12}$ . These results imply that the SCQD may have a stable  $T_0$  under small fluctuations of the QD size, and a high value of  $T_0$  can be achieved for small size QDs.

To achieve a thermal device with a high density of charge and heat currents, we need to consider a higher SCQD density. Consequently, the proximity effect between SCQDs on the Seebeck coefficient should be investigated. For simplicity, we employ the case shown in the inset of Fig. 3 as an example. The detailed expression of transmission factor for two parallel SCQDs can be found in ref. 15, where we investigated the charge ratchet effect on current rectification. Figure 3 shows the Seebeck coefficient as a function of temperature. The curves  $S_1(T)$ ,  $S_2(T)$ ,  $S_3(T)$ , and  $S_4(T)$  correspond respectively to the interdot Coulomb interaction  $U = 0, 4, 6$ , and  $8\Gamma_0$ . In Fig. 3(a), we consider  $U_\ell = 30\Gamma_0$ ,  $E_\ell = E_F - 10\Gamma_0$ , and  $U_{12} = U_{34} = 10\Gamma_0$ . In Fig. 3(b), we consider  $U_\ell = 60\Gamma_0$ ,  $E_\ell = E_F - 20\Gamma_0$ , and  $U_{12} = U_{34} = 20\Gamma_0$ . We observe that  $T_0$  is pushed toward a lower temperature with increasing  $U$ . In Fig. 3(a),  $S_4(T)$  (blue line) is negative in the entire temperature regime. Such a behavior in-

dicates that the number of resonant channels involving electron Coulomb interactions above  $E_F$  increases with increasing  $U$  and they dominate electron carrier transport. In Fig. 3(b), we obtain  $k_B T_0 = 27\Gamma_0$  in the curve of  $S_1(T)$ . Compared with the black line in Fig. 3(a),  $T_0$  is enhanced. This is attributed to the increase in intradot Coulomb interactions  $U_\ell$ . In Particular, there are two zero-crossing temperatures in the  $S_2(T)$  and  $S_3(T)$  curves. They are  $k_B T_0 = 6\Gamma_0$  and  $k_B T_0 = 22\Gamma_0$  in the  $S_2(T)$  curve, and  $k_B T_0 = 5\Gamma_0$  and  $k_B T_0 = 19\Gamma_0$  in the  $S_3(T)$  curve. The oscillatory behavior of the Seebeck coefficient in the  $S_2(T)$  and  $S_3(T)$  curves is observed. There is only one zero-crossing temperature,  $k_B T_0 = 14.5\Gamma_0$ , in the  $S_4(T)$  curve.

In this study, we find that the sign of electrochemical potential can be tuned by selecting the equilibrium temperature for a given temperature gradient. This implies that a temperature-controlled bipolar thermoelectric device can be achieved. For the two parallel SCQDs, the oscillatory behavior of the Seebeck coefficient with respect to temperature is also observed.

#### Acknowledgments

This work was supported in part by the National Science Council of the Republic of China under Contract Nos. NSC 99-2112-M-008-018-MY2, and NSC 98-2112-M-001-022-MY3.

† E-mail address: mtkuo@ee.ncu.edu.tw

\* E-mail address: yiachang@gate.sinica.edu.tw

- 
- <sup>1</sup> A. J. Minnich, M. S. Dresselhaus, Z. F. Ren and G. Chen: Energy Environ Sci, **2**, 466 (2009).
  - <sup>2</sup> G. Mahan, B. Sales and J. Sharp, Physics Today, **50**, 42 (1997).
  - <sup>3</sup> R. Venkatasubramanian, E. Siivola, T. Colpitts, B. O'Quinn, Nature **413**, 597 (2001).
  - <sup>4</sup> A. I. Boukai, Y. Bunimovich, J. Tahir-Kheli, J. K. Yu, W. A. Goddard III and J. R. Heath, Nature, **451**, 168 (2008).
  - <sup>5</sup> T. C. Harman, P. J. Taylor, M. P. Walsh, B. E. LaForge, Science **297**, 2229 (2002).
  - <sup>6</sup> K. F. Hsu, S. Loo, F. Guo, W. Chen, J. S. Dyck, C. Uher, T. Hogan, E. K. Polychroniadis, M. G. Kanatzidis, Science **303**, 818 (2004).
  - <sup>7</sup> A. Majumdar, Science **303**, 777 (2004).
  - <sup>8</sup> G. Chen, M. S. Dresselhaus, G. Dresselhaus, J. P. Fleurial and T. Caillat, International Materials Reviews, **48**, 45 (2003).
  - <sup>9</sup> Y. M. Lin and M. S. Dresselhaus, Phys. Rev. B **68**, 075304 (2003).
  - <sup>10</sup> P. Murphy, S. Mukerjee, J. Morre, Phys. Rev. B **78**, 161406 (R) (2008).
  - <sup>11</sup> David. M. T. Kuo and Y. C. Chang, Phys. Rev. B **81**, 205321 (2010).
  - <sup>12</sup> Y. Dubi, and M. Di Ventra, Rev Modern Phys **83**, 131 (2011).
  - <sup>13</sup> R. Sanchez and M. Buttiker, Phys. Rev. B **83**, 085428 (2011).
  - <sup>14</sup> N.C. van der varrt, S. D. Franceschi, J. M. Elzerman, T. Fujisawa, S. Tarucha, and L. Kouwenhoven, Rev. Mod. Phys. **75**, 1 (2003).
  - <sup>15</sup> David. M. T. Kuo, S. Y. Shiau and Y. C. Chang, arXiv 1101.5751
  - <sup>16</sup> David. M. T. Kuo, and Y. C. Chang, Phys. Rev. Lett. **99**, 086803 (2007).
  - <sup>17</sup> Y. C. Chang, and D. M. T. Kuo, Phys. Rev. B **77**, 245412 (2008).
  - <sup>18</sup> J. Fransson, and M. Rasander M, Phys. Rev. **73** 205333 (2006).
  - <sup>19</sup> J. Inarrea, G. Platero, and A. H. MacDonald, Phys. Rev. B **76**, 085329 (2007).

### Figure Captions

Fig. 1. The electrical conductance  $G_e$  and Seebeck coefficient as a function of temperature for various values of  $E_2$  (from  $E_F - 10\Gamma_0$  to  $E_F - 33\Gamma_0$ ) with  $E_1 = E_F - 10\Gamma_0$ ,  $t_C = 0.1\Gamma_0$  and  $\Gamma_L = \Gamma_R = 1\Gamma_0$ . Insets shown in Fig. 1(a) and 1(b) illustrate, respectively, the SQCD connected to the metallic electrodes and the band diagram corresponding to Fig. 1(a).

Fig. 2. Seebeck coefficient as a function of temperature at  $E_1 = E_2 = E_F - 10\Gamma_0$  for different electron Coulomb

interactions. Other parameters are the same as those of Fig. 1. Diagram (b) shows the probability of resonant channels in the case of  $U_{12} = 10\Gamma_0$ .

Fig. 3. Seebeck coefficient as functions of temperature for various values of interdot Coulomb interaction  $U_{13} = U_{24} = U$  and  $U_{14} = U_{24} = U/2$ . Diagrams (a) and (b) consider two different sets of physical parameters  $U_\ell = 30\Gamma_0$ ,  $E_\ell = E_F - 10\Gamma_0$ ,  $U_{12} = U_{34} = 10\Gamma_0$  and  $U_\ell = 60\Gamma_0$ ,  $E_\ell = E_F - 20\Gamma_0$ ,  $U_{12} = U_{34} = 20\Gamma_0$ , respectively.

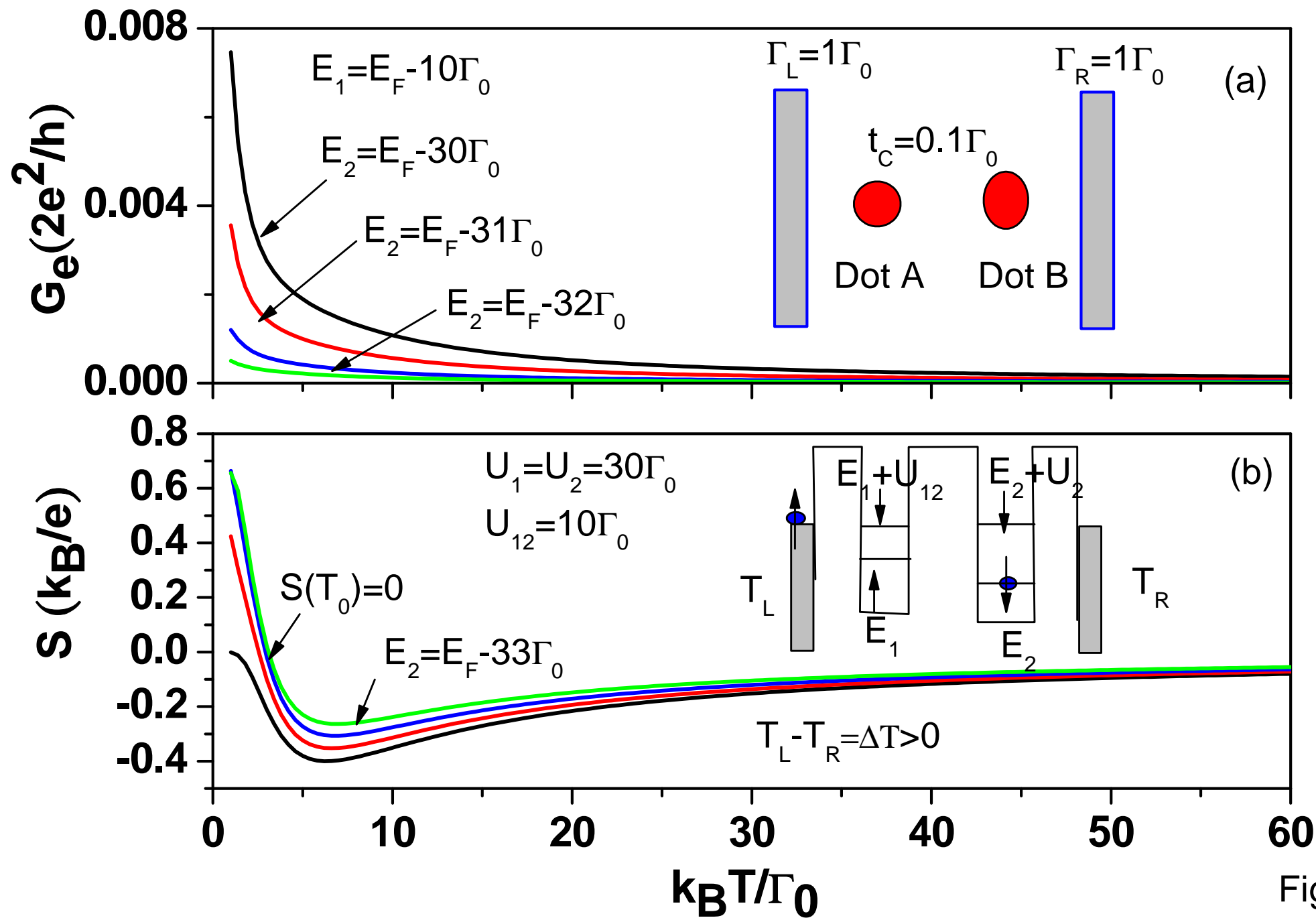


Fig1

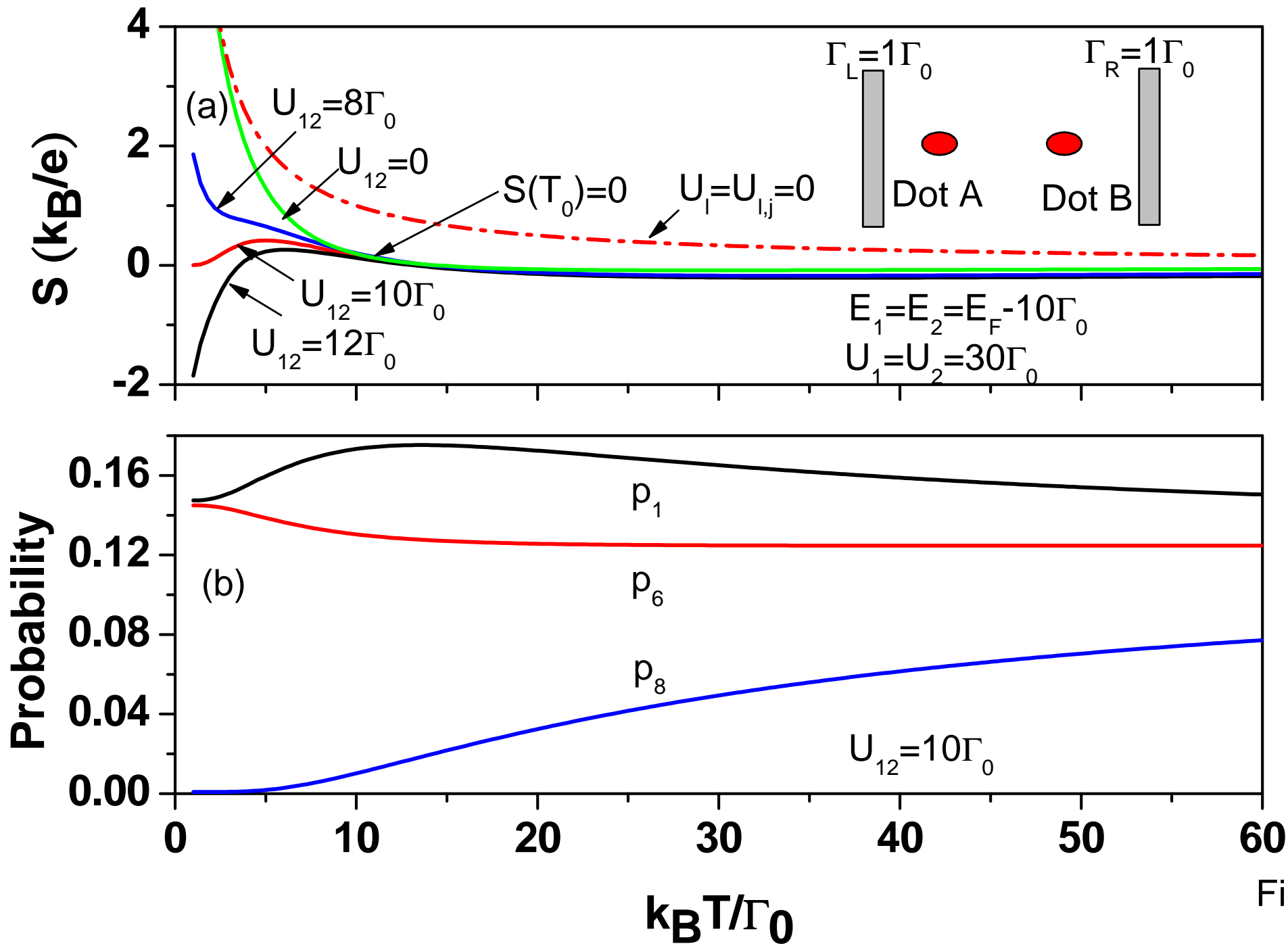


Fig2

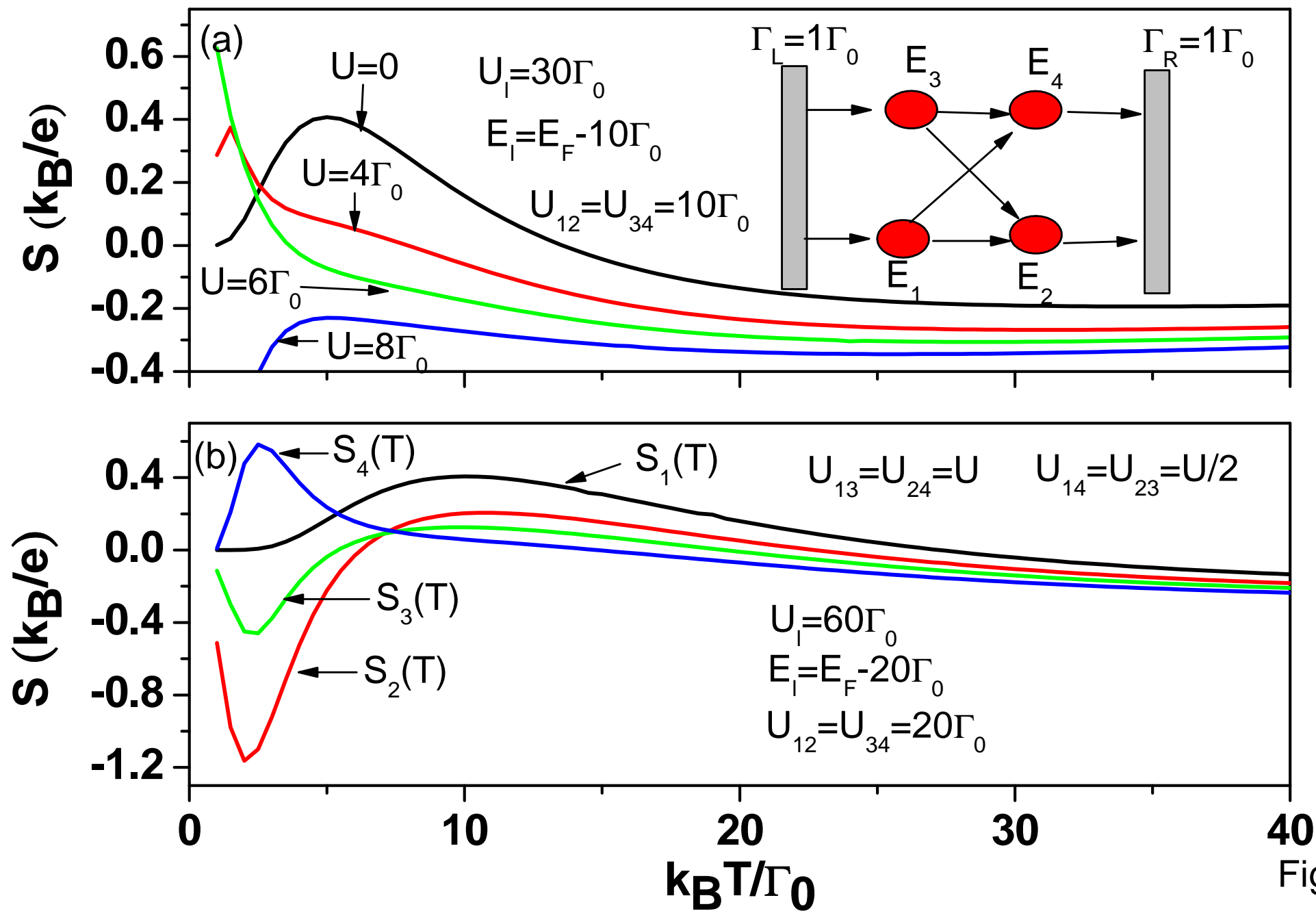


Fig3